FAILURE ANALYSIS CASE STUDY ON CONDENSER VESSELS OF GAS REMOVAL SYSTEM IN WAYANG WINDU GEOTHERMAL POWER PLANT UNIT 2

Gian Ganjar Zatnika*, Wilis Wirawan, and Stefanus Wisanto
Star Energy Geothermal (Wayang Windu) Ltd
Pangalengan, Bandung 40378, West Java, Indonesia

Abstract

Gas exhauster or gas removal system is typical facility for non-condensable gases (NCG) removal from turbine condenser in a single flash geothermal conversion system. Wayang Windu Geothermal Power Plant Unit 2 in West Java, Indonesia, which is also operated by single flash system, applies a hybrid type Gas Removal System (GRS) consisting of three exhauster series. The second-stage, direct-contact condenser vessels of those three series experienced cracks and leaks alternately after three years of operation. Material testing and examination including metallography, hardness test, and SEM-EDS analysis have been conducted to deliver failure analysis of the condenser failures. It was concluded that the cracks were caused by hydrogen cracking due to combination of corrosive environment in the vessel and high residual stress thanks to its manufacturing process. Based on this study, several improvement on material specifications and maintenance activities of surface facility equipments were proposed in order to afford more reliable geothermal power plant.

Keywords : geothermal, failure analysis, hydrogen cracking, gas exhauster, non condensable gases.

I. INTRODUCTION

Wayang Windu Power Plant has two units Power Station delivering a total of 227 MW electricity to PT Perusahaan Listrik Negara (PLN) that dispatches the electricity into the West Java transmissions grid. Wayang Windu Power Station Unit 2 generates maximum of 117 MW electricity by a single cylinder, condensing type steam turbine.

After doing work in the turbine, the steam is exhausted to and condensed in a turbine condenser. The turbine condenser is a direct contact spray type mounted beneath the steam turbine. Non condensable gases (NCG) from the condenser are collected and removed by a Gas Removal System (GRS) linked to it.

GRS is a hybrid exhauster system consisting of steam ejectors and vacuum pumps. It has function to remove NCG that accumulates as the incoming steam condenses in the turbine condenser and to deliver them to the cooling tower to be carried away in the thermal plume. The motive steam of GRS ejectors is supplied by line branched from the main steam pipe to the turbo generator. The cooling water for the GRS condensers is sourced from the cooling tower.

NCG from the main condenser flows firstly through the first stage ejectors. NCG and the ejector motive steam are mixed, condensed, and separated in the direct contact inter-condensers where the separated NCG flows through the second stage ejectors. Again, the

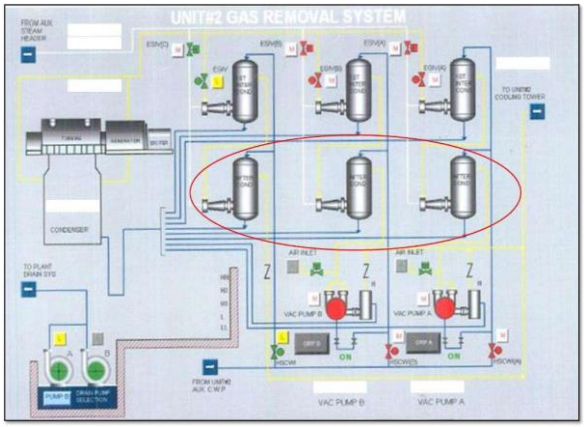

Figure 1 Gas removal system process layout diagram[1]

combined NCG and motive steam in the second stage ejectors are condensed and separated in the direct contact after-condensers. Finally, the separated NCG is extracted through the liquid ring vacuum pumps and separated at the separators. The NCG is then combined into a header and routed to the cooling tower.

Unit 2 GRS after-condenser vessels of Train A, Train B, and Train C, which are second stage direct contact condensers experienced cracks and leaks alternately after three years of operation. Failure analysis including material testing and design review have been conducted thereafter to reveal the root cause of the crack failures. Step by step process of performed failure analysis and its results are provided in this work in order to deliver technical review for future development of geothermal power plant.

*Corresponding author. Tel.: +62 852 2246 1261;
Email address: gian.ganjarzatnika@starenergy.co.id

II. DATA COLLECTION

2.1. Failure Description and Samples

Wayang Windu Unit 2 GRS consists of three trains of hybrid exhauster system. The process layout of GRS system is shown on Figure 1. Train A and B are assembled in series by first stage ejector – inter-condenser system, second stage ejector – after-condenser system, and vacuum pump – separator system. These Train A and B are operated continually. Whereas, GRS Train C which roles as back-up is only assembled by first stage ejector – inter-condenser and second stage ejector – after-condenser system with monthly operation test.

After-condenser vessel of all Train A, B, and C experienced cracks during their operation. The number and location of cracks were various for each train. However, the cracks have similar morphology and located either on base metal or on weld metal area.

Two crack samples as called sample C and sample B were disassembled respectively from after-condenser vessel C and after-condenser vessel B for material testing and failure examinations. There was no sample from after-condenser A although it also has cracks.

The samples, origin location, and existing crack appearance for after-condenser sample C and sample B are shown on Figure 2. Sample C is curved material sheet consisted of one through thickness crack located in base metal area adjacent to a fillet weld joint. The crack was coated on its outer surface side.

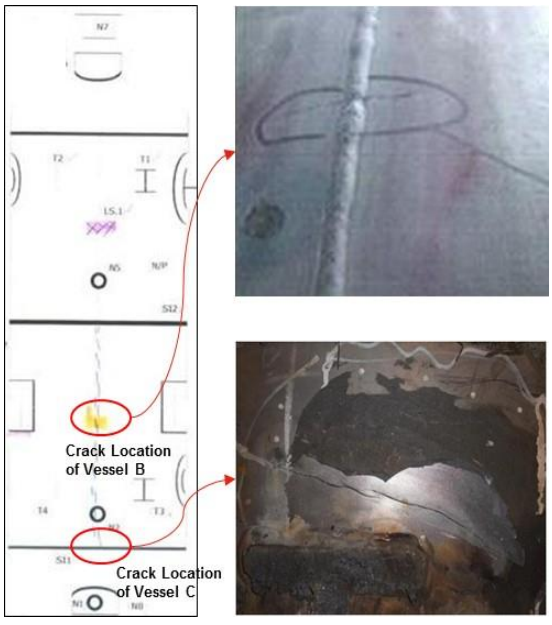

Figure 2 Crack and origin location for both examined samples.

On the other hand, sample B contains one through thickness crack perpendicular to the vessel's longitudinal seam weld joint. These samples were taken as typical crack section for base metal and weld metal area, respectively.

2.2. Material and Operational Design

Material specification and mechanical properties of vessel material are shown on Table 1. Actual and design operation data for both vessels are also presented on Table 2.

It can be seen that both condenser vessel C and vessel B are identified as low carbon grade austenitic stainless steel made from hot rolled plate with finishing by annealing and pickling process. It was also heat treated by annealing and quenching thereafter at metal temperature of 1100 ^{o}C. In terms of corrosion service, the plate was tested for intergranular corrosion resistance, but it was not tested for sulfide cracking or other environmentally induced cracking resistance.

This typical heat treatment and corrosion test usually deliver an austenitic stainless steel material having low susceptibility to intergranular corrosion by limiting sensitization during welding or operation. However, this treatment might generate material having high susceptible to environmentally induced cracking since a water quench may reintroduce high residual stresses [2].

Based on Table 2, pressure and temperature of motive steam coming from second stage ejector exceed the design criteria. However, phase equilibrium and thermodynamics condition in the vessel is unknown because of complexity of mixed operating fluids and suction pressure from vacuum pump connected to vessel's outlet. In spite of that, this low operation pressure could not be a root cause of failure regarding higher capacity of the vessels.

Cooling water for after-condenser vessel is sourced from cooling tower, whereas motive steam for after-condenser vessel is piped from auxiliary steam system. Water quality of both operating fluids for last 3 years were collected and shown on Table 3.

Water and steam quality data indicates chemical species which could be associated to the failure, i.e. Cl or H_2S. Indeed, H_2S gas is one of NCG component in addition to other residual gases. Hence, H_2S from NCG adds total H_2S content in after-condenser vessel.

Table 1 Material Specification and Properties

Description	After Condenser C	After Condenser B
Identification and Specification		
Component name	After-condenser Train C	After-condenser Train B
Material grade	SS 316L (SA240/UNS-S31603)	SS 316L (SA240/UNS-S31603)
Outer diameter	42 in	42 in
Nominal thickness	6.35 mm	6.35 mm
Delivery condition	Hot rolled coil, Finish 1D	Hot rolled coil, Finish 1D
Heat treatment	Quenched at 1100 oC (forced air + water)	Quenched at 1100 oC (forced air + water)
Performed corrosion test:		
ASTM A262-E (Intergranular Corrosion)	Yes	Yes
NACE MR0175 (Sulfide cracking)	No	No
Mechanical Properties		
Yield Strength (MPa)	310	310
Tensile Strength (MPa)	600	600
Elongation (%)	50	49
Hardness (HV)	170	170
Chemical Composition (%w)		
C	0.02	0.019
Si	0.53	0.48
Mn	1.41	1.42
P	0.032	0.031
Si	0.003	0.001
Cr	16.95	16.99
Ni	10.1	10.07
Mn	2.14	2.03
Nb	0.02	0.014
Cu	0.36	0.38
Co	0.26	0.24
N	0.047	0.043

III.TESTING AND EXAMINATION

3.1. Visual Examination

Visual examinations were carried out on both samples. Samples and crack appearance are shown on Figure 3 and Figure 4. For Sample C, the crack is adjacent to fillet weld joint for lifting lug, through thickness, and its orientation is perpendicular to axis or longitudinal direction of the vessel (Figure 3a).

For Sample B, the crack passes through the longitudinal weld seam of the vessel, through thickness, and is laid on transversal direction of the vessel as well (Figure 4a). Additionally, there is no observable corrosion or pitting attack both around the crack and on weld seam for both samples. The welding area moreover was sound and has no visual weld defect.

Fracture surface of samples was also observed from bottom head side on longitudinal surface as presented on Figure 3c and Figure 4b. For sample C, the fracture surface appearance shows major brittle fracture with little area of plastic deformation on the edge of its internal surface.

Differently, the fracture surface of sample B (Figure 4b) shows two separated weld area on its inner and outer surface. It also shows various fracture appearances i.e. smooth brittle fracture on base metal area, lightly brittle fracture on weld area, and cup and cone fracture indicating ductile fracture. Apparently, a weld defect was observed in the middle of vessel's thickness between inner and outer weld area (Figure 4b and 4d). It is likely a *lack of fusion* indicating improper weld joint design.

Table 2 Operational Parameters

Parameters	After Condenser C	After Condenser B
Motive Steam		
Operation Pressure (barg)	10.00	9.50
Temperature (^{o}C)	182.30	182.30
Cooling Water		
Operation pressure (barg)	2.25	2.25
Temperature (^{o}C)	25.88	25.88
NCG		
Operation pressure (barg)	0.65	0.65
Temperature (^{o}C)	52	52
Condenser Vessel Overall		
Operation fluid	NCG, steam, water	
Design pressure (barg)	8.18	
Design temperature (^{o}C)	175.56	

Table 3 Fluid Chemistry

Parameters	Unit	Range value
Cooling water chemistry		
pH	-	5.6-7.3
Electroconductivity	µS	143-391
Total dissolved solids	ppm	74-186
SO_4^-	ppm	45-85
B	ppm	12-22
NH_3	ppm	5-8
$CaCO_3$	ppm	4-12
HCO_3	ppm	13-28
Steam chemistry		
pH	-	4.1-4.7
SiO_2	ppm	0.1-0.11
Cl	ppm	0.1-0.2
Fe	ppm	0.1-0.11
B	ppm	1.2-2.4
H_2O	%w	98.73-99.65
Total gas content	%w	0.35-1.27
CO_2	%w	0.33-1.23
H_2S	%w	0.02-0.04

Based on visual examination, the crack location and orientation might be associated to welding process during vessel fabrication either fillet weld for vessel C or longitudinal seam weld for vessel B. Moreover, its orientation indicates that the crack is more affected by stress on longitudinal direction instead of hoop direction.

Refer to the fracture surface appearance; cross section of vessel thickness must be subjected to inhomogeneous or localized stress pattern. Especially for vessel B, the crack might be initiated from weld defect, propagated to both sides, and terminated at cup and cone fracture site [3].

3.2. Metallography Examination

3.2.1. After Condenser C

Metallography examination of sample C was carried out at base metal and several part of the crack. For base metal, specimen was viewed perpendicular to inner surface and also from

longitudinal cross section. On the other hand, crack specimens were viewed perpendicular to inner surface. The metallography specimen of sample C and its key results are presented on Figure 4.

Base metal

It can be verified from base metal sample that material constituent is equiaxed austenite phase (Figure 3e). The observation also reveals several metallurgical features. Firstly, base metal has inhomogeneous austenite grain size. Moreover, it has no observable carbide, but contains several twin structures at numerous random spots.

In addition, there are several areas with ferrite phase stringers aligned the rolling direction (transversal direction of vessel). It is typical that alloys with low carbon contents as the sample will have a greater tendency toward δ-ferrite stabilization [4].

These aforementioned features could indicate improper manufacturing or heat treatment of vessel. Especially for the ferrite stringer, it might affected by plate rolling or welding process during fabrication [5].

Crack area

Crack material samples were taken apart from the whole crack area. Macrophotograph of polished-etched surface shown on Figure 3b reveals that the cracks are laid separately each other. In other words, the crack propagates in stepwise, not in straight manner.

Furthermore, numerous micro cracks were observed between larger cracks. These micro cracks were then examined microscopically and presented on Figure 3d, 3f, and 3g. All of the cracks are propagated on transversal direction i.e. parallel to rolling direction of the vessel. It might be associated with the presence of ferrite stringer which is also laid parallel to the rolling direction and could predominantly be a crack initiation site [6].

Further examination of microstructure around micro cracks shows that all cracks are mostly transgranular type and have generated branching at several points as shown on Figure 3f and 3g. These branching cracks indicate high stress level involved in crack growth. It can also be observed that the crack is propagated following finer grain size or twin structure, which is confirmed by the hardness test result herein, that those structure are more brittle than the other common microstructure constituents.

3.2.2. After Condenser B

Metallography examinations of sample B were carried out at 2 location of weld metal: 1 specimen at area without crack and 1 specimen at crack area. The specimen without crack was viewed from longitudinal cross section (4d); the crack specimen was viewed perpendicular to inner surface (Figure 4c). The metallography specimen of sample B and its key results are presented on Figure 4.

Weld area without crack

The weld sample consists of two weld metal area at inner and outer wall surface on austenitic phase base metal (Figure 4d). It can be seen that material also contains phase stringers (Figure 4e). Its distribution is more likely found around weld metal developing a banded structure, a metallurgical feature which is usually emerged due to welding process [7].

Apparently, it is also observed a crack-like weld defect which is likely *lack of fusion* pass through the thickness from both of weld root area (Figure 4b). This defect is typically developed as a result of inappropriate weld joint design and would be obviously correlated with the crack development in after-condenser B.

Crack area

Microstructure around crack area on the weld metal is presented on Figure 4f. Both macro and microphotograph of crack on the sample B show some similar features with crack on sample C. The cracks are also transgranular and has generated branch indicating excessive stress level involved.

This branching crack is more likely found on weld area where typically high residual stresses are presented [5]. Stepwise micro cracks are also existed in addition to the larger one.

These similarities lead to supposition that crack growth on sample B has similar manner with crack on sample C although it is taken place on welding area.

3.3. Hardness Test

Hardness test was conducted by Micro-indentation Vickers method based on ASTM E-384. For Sample C, the specimen was taken from metallography sample C covering test spots: base metal area, area at crack bank, area between cracks, and crack area passing twin structures. For Sample B, the test covers base metal area, HAZ area, weld metal area, and area at crack bank. The testing result and ASME standard of hardness are presented in Table 4.

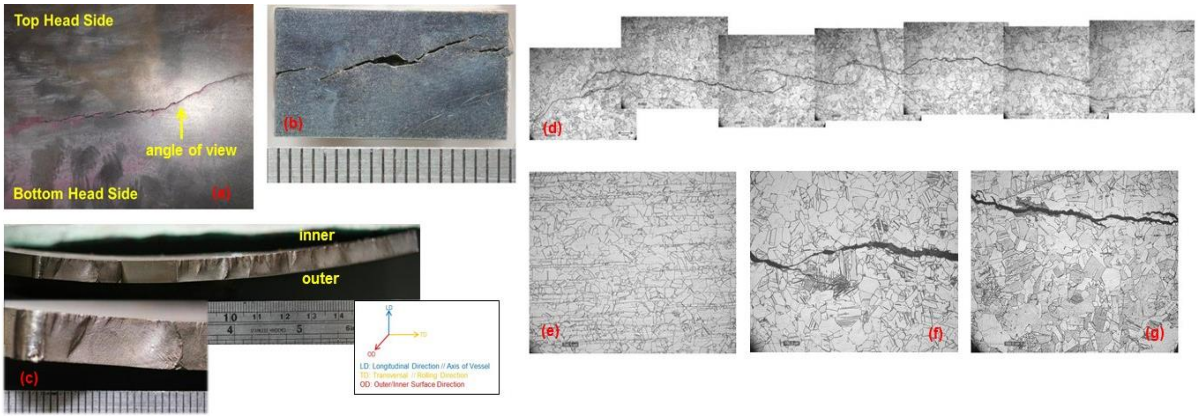

Figure 3 Fractography and metallography results of sample C: *(a)* as-received crack sample; *(b)* metallography sample cut from *a*; *(c)* longitudinal fracture surface viewed from bottom head side; *(d)* microphotograph of crack showing transgranular, stepwise crack; (e) microphotograph of base metal containing ferrite phase stringer; *(f) & (g)* crack section of *d* with higher magnification showing crack on twins and branching.

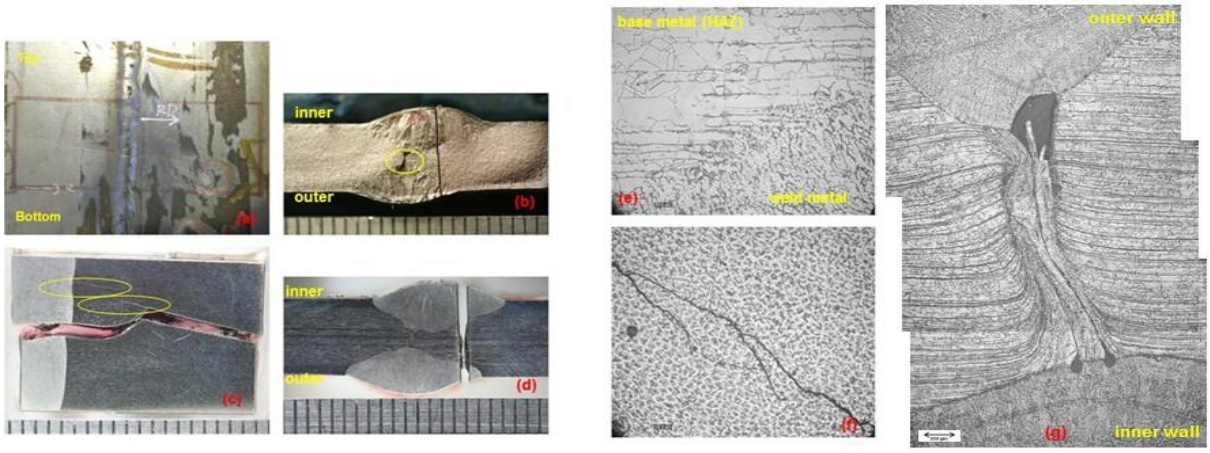

Figure 4 Fractography and metallography results of sample B: *(a)* as-received crack sample; *(b)* longitudinal fracture surface viewed from bottom head side; *(c) & (d)* metallography sample cut from *a*; *(e) & (f)* microphotograph of weld metal including branching crack therein; and *(g)* microphotograph of weld defect.

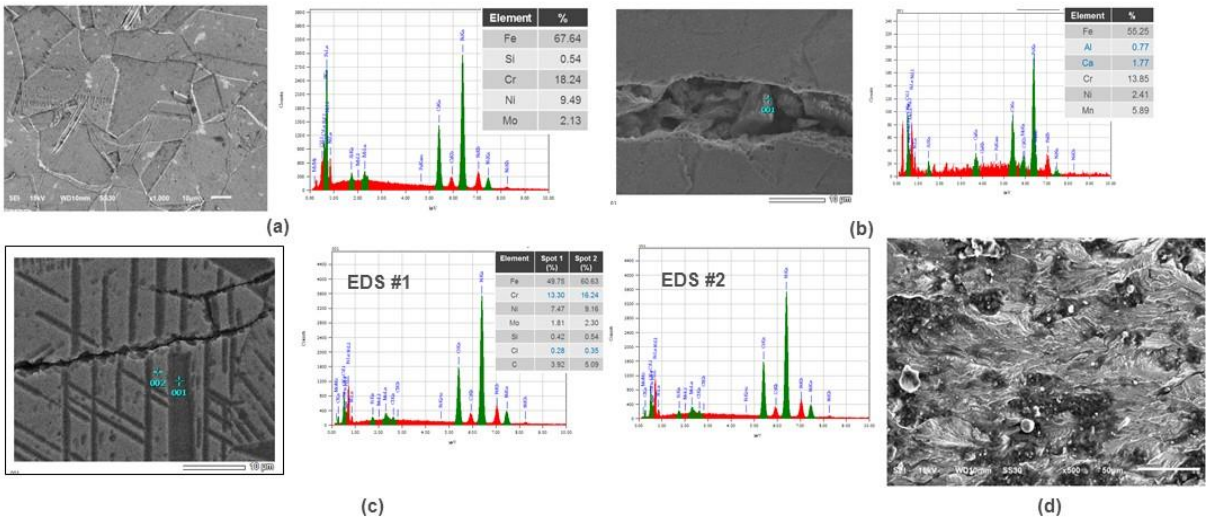

Figure 5 SEM and EDS examination result: *(a)* base metal overall; *(b)* nonmetallic inclusion on the crack path; *(c)* twin structure at crack vicinity *(d)* electron microscophy of fracture surface at weld area.

Table 4 Hardness Test Result

Spec Code.	Area	Area Code	Hardness (HV 0.2)
C3	Base metal away from crack	1	200
	Crack bank	2	231
	Area between cracks	3	256
	Crack area with Twins	4	256
B1	HAZ area	5	220
	Weld metal	6	220
B2	Base metal away from crack	7	200
	Crack bank	8	210
ASME Sec. IIA - SA 666 Specification*			217 HV max.

Testing result for sample C

Based on Table 4, hardness for base metal area of sample C are still under ASME compliances. Nonetheless, measurement on the other spots around crack area gives higher values which do not comply with the specification. Hardness at crack bank is slightly higher than base metal hardness with maximum value exceeds 217 HV (recommended maximum hardness).

Furthermore, hardness at area between cracks and at crack area with twin structures are far higher up to 256 HV. High hardness level on several local spots around crack could indicate brittleness and reduction of toughness. In other words, it indicates embrittlement process either caused by corrosive environment during operation or by welding process during vessel fabrication [5].

Testing Result for Sample B

Hardness at crack bank of sample B are slightly higher than base metal, but it is not as high as hardness values at crack bank of sample C. In conjunction with that, hardness of weld metal is slightly higher than base metal but it is still in range with the specification. It indicates that crack growth is more influenced by high hardness constituent or structure area associated to welding process instead of weld microstructure itself.

3.4. SEM and EDS Examination

SEM and EDS examinations were carried out from material sample C covering base metal matrix and crack area. For Sample B, only fractography analysis by SEM examination was carried out onto its fracture surface. The results are shown on Figure 5 and summarized on Table 5.

Table 5 Phase and Deposit Analysis Result

Location	Element (%w)								
	Si	Cr	Ni	Mo	Mn	Ca	Al	Fe	Cl
Base Metal Overall	0.54	**18**	9.49	2.13	-	-	-	67.64	-
Inclusion on Crack Path	-	**14**	2.41	2.2	**5. 89**	**1.8**	**0.8**	55.25	-
Twins around the Crack:									
Spot #1	0.42	**13**	7.47	1.81	-	-	-	49.75	**0.3**
Spot #2	0.54	**16**	9.16	2.3	-	-	-	60.63	**0.4**
Raw Material	0.53	**17**	10.1	2.14	1.41	-	-	Balance	**-**

Phase Analysis of Sample C

Spectroscopy result of base metal area of sample C on Table 5 gives typical result with heat analysis of raw material of after-condenser C on Table 1, except for higher Cr content on the sample up to 18.24 %. This higher Cr content can describe the presence of ferrite stringer on sample microstructure providing that Cr roles a ferrite promoter [5].

Apparently, SEM and EDS analysis on crack path has discovered calcium and aluminum content which is likely come from a nonmetallic inclusion in microstructure of stainless steel [4]. These inclusions could be the predominant initiation sites for cracking especially for those which has stepwise manner [6, 8].

Furthermore, analysis on twin structure at vicinity of the crack shows valuable information. Firstly, Cr content reduces up to 16.24 % and 13.30 % for spot #1 and spot #2, respectively. Secondly, on those Cr-reduced spot, it is observed Cl species which might also be the cause of Cr reduction process [9]. The presence of Cl is consistent with operational data verifying that steam consists of this aggressive species for stainless steel.

Fractography Analysis of Sample B

Fractography results by means of SEM on sample B are presented on Figure 5d. From that result, it can be observed that weld metal fracture surface is more ductile than base metal one. In addition, fractography of base metal fracture surface shows river marking which could indicate crack propagation orientation [3].

Based on those finding it can be concluded that weld metal structure has no or little influence on crack development. Instead, the *lack of fusion* defect on base metal can increase susceptibility of this material to have brittle fracture as result shown [6].

IV. SUMMARY OF ANALYSIS

4.1. Testing Results and the Root Causes

Low carbon grade austenitic stainless steel material of after-condenser vessel C and vessel B in Wayang Windu Power Plant complies with ASME Sec. IIA – SA-666 specification in terms of mechanical testing and heat analysis. Moreover, operating conditions of both vessels comply with its design. Nonetheless, operating fluids are occupied with Cl and H_2S which have detrimental effect to stainless steel.

Visual examination, metallography examination, and SEM-EDS analysis on crack area of sample C and sample B show that

cracks are mostly transgranular, propagated in stepwise manner on rolling direction aligned with ferrite stringers, and occupied with nonmetallic inclusion. In addition to that, hardness test result strongly indicates that after-condenser material experienced embrittlement especially at the crack vicinity. Those aforementioned symptoms demonstrate that after-condenser material has susceptibility to hydrogen cracking phenomena.

In addition, visual examination and metallography analysis show inhomogeneous grain size, excessive twin structure, and ferrite stringers on sample C as well as *lack of fusion* defect and ferrite stringers on sample B. Those microstructural features can also increase susceptibility to hydrogen attack. Those might be caused by improper manufacturing process, heat treatment, or welding processes [5].

Naturally, austenitic stainless steels are not susceptible to hydrogen cracking or any other environmentally induced cracking [10]. However, this exclusion can be possibly found due to aforementioned metallurgical factor and environmental condition. Indeed, EDS analysis on crack vicinity of sample C shows Cl content on material surface indicating corrosion attack introduced by chloride. This corrosion process can break passive layer of material and induce hydrogen attack thereafter [9].

Apart from that, metallography analysis also shows that all cracks have developed branching which indicates high stress level involvement on crack growth. According to orientation of all the cracks, it can be inferred that longitudinal stress, which either applied or residual stress, is more predominantly contributed to crack development [3].

Based on the crack locations, it is intangible to analyze that operational applied stress could crack those locations. Therefore, the crack growth could more be affected by residual stress. Regarding all the cracks are located either near to or on welding joint and material was not stress relieved, residual stress might be generated from welding or manufacturing process.

Stress affecting the cracks might also be come from pressure accumulation of hydrogen gases within material. It is common that hydrogen induced cracking mechanism can build such an internal pressure that adds other applied or residual stress to crack the material [6]. This mechanism is explained further on section 4.3.

To summarize, the cracks on after-condenser vessels were caused by hydrogen cracking due to combination of corrosion process and high residual stress. Corrosion and hydrogen damage may be caused by corrosive environment such as Cl and H_2S content in operating fluids.

Moreover, it might be enhanced by metallurgical factor inducing corrosion-cracking susceptibility such as ferrite stringer, nonmetallic inclusion, weld defect, and embrittlement phenomena at crack vicinity. Weld defect in sample of after-condenser B is unacceptable and strongly contributed to crack growth since it might be a crack initiation site.

In addition to that, the examination strongly reveals that high stress level occurred on the after-condenser. Residual stress emerged from manufacturing and/or welding process could be contributed to develop such stress level that would assist hydrogen cracking mechanism.

4.2. Austenitic Stainless Steel 316L and Susceptibility to Corrosion Cracking

Austenitic stainless steel has an austenitic structure which stable at room temperature. Depending on ratio of ferrite-promoting elements to austenite-promoting elements, its microstructure will be either fully austenitic or a mixture of austenite and ferrite. This material was developed for application requiring better atmospheric or elevated temperature corrosion resistance with strengths equivalent to those of mild steels [5].

UNS-S31603 material or known as SS 316L is special grade of austenitic stainless steel designed to obtain better resistance to pitting corrosion and intergranular corrosion. It can be obtained by adding Mo up to 2% and lowering C up to 0.03% respectively to conventional austenitic stainless steel design of SS 304.

Having good properties on pitting and intergranular corrosion resistance does not make this material resist to chloride stress corrosion cracking (SCC) and in some circumstance to hydrogen induced cracking (HIC) or sulfide stress corrosion cracking (SSC). Austenitic stainless steel is highly resistant to those environmentally induced cracking in annealed condition but can become quite susceptible when heavily cold worked or improperly heat treated [6].

Fastinatingly, quenching treatment for avoiding intergranular corrosion could introduce residual stress which makes the material more susceptible to stress corrosion. In general

application, this susceptibility of steel or other metallic materials to Stress Corrosion Cracking (SCC), Hydrogen Induced Cracking (HIC), or Sulfide Stress Cracking (SSC) is usually tested according to each testing standard i.e. ASTM G139 for SCC, NACE TM0284 for HIC, and NACE TM0177 for SSC.

4.3. Hydrogen Induced Cracking Mechanism on After – Condenser

Refer to Table 1, stainless steel material for after-condenser vessels were heat treated by annealing and quenching. Consequently, it would be resistant to intergranular corrosion. However, this material was not heat treated intentionally for stress release and not tested for any of environmentally induced cracking tests. Hence, it can be suspected that construction material of after-condenser is susceptible to corrosion cracking.

Indeed, all laboratory testing and examinations prove that this material is susceptible to corrosion cracking. Therefore, it can be concluded that all cracks on sample C and sample B are caused by kind of environmentally induced cracking phenomena. In case of sample B, *lack of fusion* defect can trigger the phenomena so that crack might develop easier. Due to its characteristic, the cracks on sample C and sample B could be categorized as crack caused by HIC instead of SCC. However, Cl could still role as predominant factor anyway although it is usually associated with SCC mechanism.

In this case, Cl that found at crack vicinity of sample C could role as passive layer breaker [9]. As passive layer break, hydrogen attack mechanism can take place which is characterized by embrittlement at the crack vicinity. Hydrogen source for this process could come from dissolved H_2S on cooling water fluid in after-condenser.

Corrosion process on internal surface of after-condenser could generate hydrogen atom which can penetrate to material lattice. Then, it could be accumulated at several kinds of hydrogen trap, for instance weld defect, inclusion, or high hardness microstructure site. Accumulated hydrogen atom then could be converted to hydrogen gas which can build localized internal gas pressure. This mechanism could be continually occurred up to such pressure that could initiate and propagate the crack [6].

V. CONCLUSION

A comprehensive methodology consisting material testing, examination, and design review have been performed for failure analysis of crack occurrences on GRS after-condenser in Wayang Windu Geothermal Power Plant Unit 2. These methods deliver a set of evidences to explicate that the cracks were caused by hydrogen induced cracking due to combination of corrosive environment and high residual stress.

Based on this failure analysis case study, it is revealed that GRS operation is subjected to corrosive conditions conducive to hydrogen cracking or other environmentally induced cracking in addition to intergranular corrosion failure mode. However, GRS in Wayang Windu is incompatible since this material is selected and heat treated only for intergranular attack consideration.

Apart from the GRS case, it is also remarked that almost all facilities on geothermal operation is subjected to sour corrosive condition due to hydrogen sulfide environment from production fluid. Therefore, power plant design against this failure mode should also be considered especially for equipment using stainless steel or other high strength alloys.

The presence of hydrogen sulfide is unavoidable in typical geothermal operating condition although it has detrimental effect to applied material. Consequently, additional design consideration shall be taken in order to take avoiding action toward hydrogen sulfide related failure. These following design consideration of surface facility material are proposed to be taken in order to afford more reliable geothermal power plant.

1. Raw material for condenser or other vessels shall be heat treated by stress relieve instead of annealing process only.
2. In addition to mechanical and metallurgical test, the material shall be corrosion tested in order to evaluate its cracking resistance in H_2S environment. Several testing method has been well established to be performed, for instances test procedure specified on NACE TM0284, and NACE TM0177.
3. Welding procedure specification and its implementation should be tightly controlled in order to avoid weld defect which may assist corrosion cracking mechanism.
4. Periodic inspection for crack detection should be performed by means of non-destructive test.

VI. ACKNOWLEDGEMENT

All of works reported herein was performed at Metallurgy and Material Engineering Laboratory of Institut Teknologi Bandung as collaboration with Star Energy Geothermal (Wayang Windu) Ltd. Accordingly; please allow me to grant my salutation to each member of Laboratory Staff and Star Energy Facility Department for all their support and contribution.

I also desire to dedicate my acknowledgment of gratitude toward the work contributors. Firstly and foremost, I would like to thank Pak Heribertus Dwiyudha and Pak Djamaludin Kurniadi for the opportunity and encouragement of this work. Also, I sincerely thank to Dr. Ir. Hermawan Judawisastra as author's adviser for plenty of admonition as well as valuable life lesson.

VII. REFERENCES

1. SEGWWL. *Internal Specification, Design, Manual and Reports*. 2014.
2. ASM Handbook, *Heat Treating of Stainless Steels*, Vol. 4, Ed.10th. 2002.
3. Barsom, J. M., *Fracture and Fatigue Control in Structures,* 1987.
4. ASM Handbook, *Metallography and Microstructures of Stainless Steels and Maraging Steels*, Vol.9. 2002.
5. Lippold, J. C. and Damian J.K., *Welding Metallurgy and Weldability of Stainless Steels*, 2005.
6. Revie, R. W., *Uhlig's Corrosion Handbook*., 2000.
7. Colangelo, V. J., *Effect of Ferrite on the Mechanical Properties of a Precipitation Hardening Stainless Steel*, 1964.
8. Robinson, S.L., B.P. Somerday, and N.R. Moody, *Hydrogen Embrittlement of Stainless Steels*.
9. Jones, D. A., *Principles and Prevention of Corrosion,* 1992.
10. M.G Fontana. *Corrosion Engineering.* 1987.
11. ASM Handbook, *Failure Analysis and Prevention*, Vol. 11, 2002.
12. ASME Sec. VIII, Div. 1, *Rules for Construction of Pressure Vessels*.
13. Yang, B. Y., C.M. Kim, and K. B. Kang, *Development of High Strength Hot Rolled Steel Strip for Sour Service,* Pohang: Corrosion Paper , Vol. No.05110, 2005.
14. Schroder, J., V. Schwinn, and A. Liessem, *Recent Development of sour service line pipe steels,* Germany: TMS (The Minerals, Metal & Materials Society).
15. Kittel, J., V. Smanio, M. Fregonese, L.Garnier, and X. Lefebvre. *Hydrogen induced cracking (HIC) testing of low alloy steel in sour environment: Impact of time of exposure on the extent of damage,* Solaize : Elsevier, 2010.
16. Davis, *Alloying Understanding The Basics,* Ohio: ASM International, 2001.